Improved Detection of Rough Defects for Ultrasonic Non-Destructive Evaluation Inspections Based on Finite Element Modelling of Elastic Wave Scattering

James R. Pettit, Anthony E. Walker, and Michael J. S. Lowe,

***Abstract*—Defects which possess rough surfaces greatly affect ultrasonic wave scattering behaviour, usually reducing the magnitude of reflected signals. Understanding and accurately predicting the influence of roughness on signal amplitudes is crucial, especially in Non-Destructive Evaluation (NDE) for the inspection of safety-critical components. An extension of Kirchhoff theory has formed the basis for many practical applications; however, it is widely recognised that these predictions are pessimistic owing to analytical approximations. A numerical full field modelling approach does not fall victim to such limitations. Here, a Finite Element (FE) modelling approach is used to develop a realistic methodology for the prediction of expected back-scattering from rough defects. The ultrasonic backscatter from multiple rough surfaces defined by the same statistical class is calculated for normal and oblique incidence. Results from FE models are compared with Kirchhoff theory predictions and experimental measurements in order to establish confidence in the new approach. At lower levels of roughness excellent agreement is observed between Kirchhoff theory, FE and experimental data, whilst at higher values the pessimism of Kirchhoff theory is confirmed. An important distinction is made between the total, coherent and diffuse signals and it is observed, significantly, that the total signal amplitude is representative of the information obtained during an inspection. This analysis provides a robust basis for a less sensitive, yet safe, threshold for inspection of rough defects.**

***Index Terms*—Finite Elements, Rough defects, Ultrasonics**

I. Introduction

DEFECTS which possess rough surfaces can greatly affect ultrasonic wave scattering behaviour and, in particular, significantly reduce the signal amplitude compared to that of a smooth defect. In Non-Destructive Evaluation (NDE), it is essential that there is a reliable method of defect detection and characterisation for the inspection of safety-critical components. Therefore, understanding and accurately predicting the influence of roughness on signal amplitudes is crucial.

A variety of analytical techniques have been developed to understand the effects of roughness on ultrasound such as the Perturbation approach [1], [2], the Rayleigh method [3], [4], and Kirchhoff theory. Kirchhoff theory is perhaps the most robust analytical technique and has been the tool of choice for modelling elastodynamic scattering problems, for both simple geometrical scatterers [5]–[8] and complex geometrical scatterers [9]–[13]. However, it has been widely recognised that these approaches are very conservative, often over estimating signal attenuation, especially for high levels of roughness. In a practical situation, these results can lead to problems with overly sensitive inspections and consequent false call problems. These conservative model predictions arise from the assumptions made when using analytical approaches, preventing them from providing accurate solutions to the complex defect geometry. This point is discussed by Zhang $et\ al$ [14], for considering the effects of roughness on sizing rough defects when using ultrasonic arrays.

A numerical method, such as a Finite Element (FE) model, does not have the same limitations as an analytical technique. FE offers the potential to calculate a full and accurate elastic wave solution for the scattering from rough surfaces, with the only limitation being computational resource that can be allocated to solving the problem. The consideration of numerical methods has become increasingly viable through the development of absorbing boundary techniques [15]–[20] and domain linking algorithms [21]–[23], allowing the spatial domain to only consider the area immediately surrounding the defect. The FE method has been successfully used to model the response from simple geometric defects such as Side Drilled Holes (SDH) and smooth cracks [24], [25], and based on the success of these methods, extensions have been made to complex defect geometries [13].

In this paper, results are presented for more complex defect geometries and rough surfaces. FE models are used to calculate the elastic scattering from multiple realisations of defects within a statistical class of roughness for normal and oblique incidence. Results from FE models are compared with Kirchhoff theory predictions and experimental measurements in order to establish confidence in the new approach. An important distinction is made between the total, coherent and diffuse signals and how they relate to scattering responses observed in ultrasonic NDE inspections. This will provide a much more accurate prediction for the attenuation due to defect roughness, aiding in establishing accurate thresholds for inspecting safety-critical components.

Manuscript submitted for review May 2015. J. R. Pettit (e-mail: jrp06@imperial.ac.uk) and M. J. S. Lowe (e-mail: m.lowe@imperial.ac.uk) are with the UK Research Centre for NDE, Imperial College London, Exhibition Road, London, UK, SW7 2AZ. A. E. Walker (e-mail: Tony.Walker@Rolls-Royce.com) is with Rolls-Royce Nuclear, PO BOX 2000, Derby, UK, DE21 7XX.

II. Rough surfaces and scattering signals

The nature of a rough surface implies that no two are ever the same. It is therefore necessary to characterise defects by a set of common surface statistical parameters such that any rough defect can be assigned to a statistical class. It has been noted from experimental measurements that the variation in height of the rough surface follows a distribution that is close to Gaussian [26], [27], where the root-mean-square (rms) height of the defect surface, σ, represents the variation in height of the defect from its mean plane. An approach making use of this observation and the resulting statistical characteristics has been widely adopted in previous studies and will be used here. The following paragraphs summarise the methodology.

The surface profile is two-dimensional, here the variation in height is defined to be in the y-axis, the defined rough surface profile runs along the x-axis, with any variations always remaining perpendicular to the z-axis (physically appearing corrugated or rutted). The function defining the surface is given by (1).

$$y = h(x) \tag{1}$$

Where h is the height deviation from the plane $y = 0$, the mean plane passing through the rough surface defined by (2).

$$< h >= 0 \tag{2}$$

Assuming Gaussian surface statistics, the surface can therefore be characterised by (3).

$$p(h)dh = \frac{1}{\sigma\sqrt{2\pi}} exp\left[-\frac{h^2}{2\sigma^2}\right] dh \tag{3}$$

Where $p(h)$, is the probability of the surface being at height between h and $h + dh$ for a given surface rms, σ. Because the FE model used to represent the surface will be spatially discretised, the rough surface must be represented by discrete spatial values. Rather than the continuous function given by (3), a discretised equivalent must be used which gives the probability density function for the height of a single discrete point on the surface, y_i, (4).

$$p(y_i) = \frac{1}{\sigma\sqrt{2\pi}} exp\left[-\frac{y_i^2}{2\sigma^2}\right] \tag{4}$$

The subscript i represents incremental changes along the x-axis, separated by an element width [11]. A second parameter is required to describe the characteristics of the roughness in the direction along the profile (x) of the surface. This is the correlation length and can be characterised by use of a correlation function, described by Ogilvy [4], (5).

$$C(R) = \frac{< h(r)h(r+R) >}{\sigma^2} \tag{5}$$

The distance over which the correlation function, $C(R)$, falls by $\frac{1}{e}$ is called the correlation length, λ_0. By defining surfaces in this manner the statistical nature of the surface can be directly related to the scattering behaviour.

For an infinite crack, the scattered ultrasonic wave can be defined by two components, termed the coherent and diffuse fields [10]. The coherent field is the same and in constant phase for all rough surfaces from the same statistical class and is located in the specularly reflected direction. The diffuse field is the random component of the ultrasonic signal which is introduced by the correspondingly random nature of the rough surface and contributes to the field in all scattering directions; this remains incoherent with respect to scattering signals from multiple realisations of surfaces within the same statistical class. These concepts are illustrated in Fig. 1.

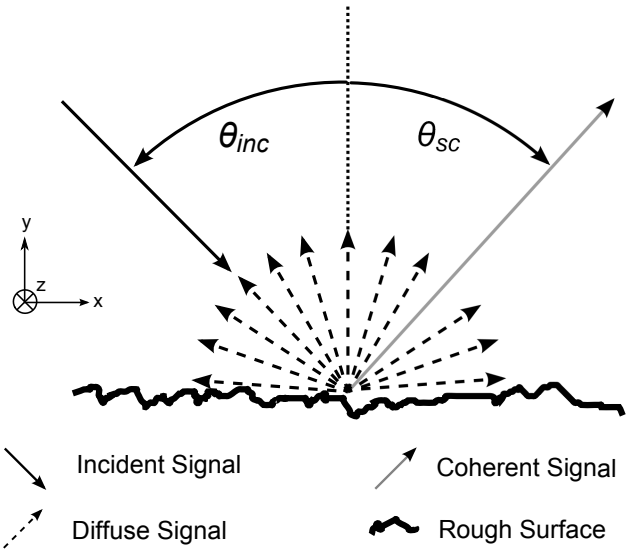

Fig. 1: Scattering of waves from a crack-like defect with a rough surface. For an infinite crack, the scattered field is shown separated into coherent and diffuse components. The coherent field lies in the specularly reflected direction such that the magnitude of the incident angle, θ_{inc}, equals the magnitude of the scattering angle, θ_{sc}. The diffuse field has a component in all scattering directions. The total field that is measured at any scattering angle from a specific rough surface is therefore comprised of the components from the coherent and diffuse fields.

When making measurements of waves scattered from rough defects, it is first necessary to make the assumption that the response from an infinite crack can be approximated to the response from a large crack, whereby the extent of the defect surface is greater than the beam width. By considering this assumption, the total signal received at any scattering angle, for a specific rough surface, is therefore comprised of a component from the coherent signal (which is common to all rough surfaces with the same surface statistics and lies in the specular direction) and a component of the diffuse field (specific to surface under consideration and has a component in all scattering directions).

An important distinction must be made between these fields and the, commonly referred to, specular signal. The specular signal is that which is observed in the specular (or mirror-like) direction. For rough surfaces, this is comprised of the whole of the coherent signal and a contribution from the diffuse field.

Since the coherent signal is in-phase for all realisations of the same statistical class, it must lie in the specular direction only. Parts of the wave that scatter away from the specular direction are random and therefore diffuse.

Currently, in industrial practice in the power generation industry, predictions of the backscattered signals from rough defects are generally made through an extension of Kirchhoff theory provided by Ogilvy [10]. For this reason, the numerical models developed here will be compared directly to findings from Kirchhoff theory in order to confirm the equivalent performance of both approaches under conditions when Kirchhoff theory is known to be accurate, and demonstrate the advantage of using the FE approach when the surface characteristics are out of range of Kirchhoff theory.

A. The application of Kirchhoff theory

The application of Kirchhoff theory to the prediction of back-scattered signals by Ogilvy [10], has resulted in the derivation of a single expression for the reduction in coherent ultrasonic signal amplitude due to increasing defect roughness, (6).

$$\frac{|\phi^{\sigma}_{coh}|}{|\phi^{\sigma=0}_{coh}|} = exp\left[-\left(k_{inc}cos\theta_{inc} + k_{sc}cos\theta_{sc}\right)^2 \frac{\sigma^2}{2}\right] \qquad (6)$$

The magnitude of the coherent signal, $|\phi^{\sigma}_{coh}|$, is a function of σ, the rms height of the defect surface, and k_{inc} and k_{sc}, the wavenumbers of the incident and scattered signals in directions θ_{inc} and θ_{sc} respectively. The magnitude of the coherent signal is normalised against $|\phi^{\sigma=0}_{coh}|$, the magnitude of the coherent reflected signal from a smooth surface.

Unlike a more general Kirchhoff formulation in which an arbitrary surface can be discretised into facets [28], the expression given in (6) is for a particular, simplified, formulation of Kirchhoff that is limited to a number of fundamental assumptions. These translate to a solution in the far-field of the defect, from an incident plane wave scattering from an infinitely wide rough surface (i.e. no crack tips), described by a Gaussian distribution of roughness, for instances where the scattering can be assumed to be independent of the correlation length.

Fig. 2 shows the predicted attenuation of the reflected coherent signal amplitude, due to increasing roughness σ, for a normally incident plane wave with wavelength λ_{inc}, expressed as a function of the incident wavelength and normalised against the response from a smooth surface [10].

As defect roughness increases, the magnitude of the coherent signal that is scattered from the rough surface is reduced. The expression given by (6) represents the reduction in the coherent signal only. It is not possible to calculate an exact expression for the diffuse signal amplitude due to its incoherent nature. However, an approximate calculation that takes the average field intensity is used to give an order of magnitude estimate. This partly explains the reason for highly pessimistic predictions for reduction in signal amplitude made using this expression, since the total field signal amplitude is not considered.

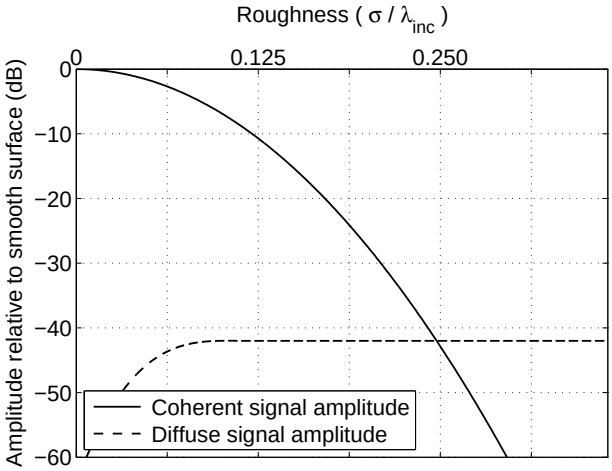

Fig. 2: Amplitude of the coherent and diffuse signals when compared to a smooth surface, for a normal incident plane wave with wavelength λ_{inc}, scattering from a defect with surface roughness, σ, as predicted by Kirchhoff theory [10].

The amplitude of the reflected field given by (6) is not sensitive to the correlation length, λ_0. Equation (6) is applicable to scenarios where the correlation length, λ_0, is such that the profile of the rough surface remains ergodic, and must therefore be small in comparison to the extent of the surface. The results presented in Fig. 2 assume an infinite rough surface making the results independent of the correlation length. For the purpose of NDE, finite sized defects with rough surfaces by their very nature will be ergodic. Furthermore, the width of the field from the transducer will typically be much larger than the correlation length of the defect. Therefore, the independence of correlation length is a valid assumption for this application.

B. The Finite Element model

Using a FE model overcomes the limitations of applying Kirchhoff theory and it is possible to calculate both the coherent signal and the total scattered field, by performing multiple simulations of the scattering from different surface realisations that satisfy the same statistical description. The results for the coherent field can then be compared against predictions for coherent signal amplitude obtained using Kirchhoff theory.

In order for a fair comparison to be made between the FE and Kirchhoff theory solutions it is important that the FE model is defined to represent the same setup that was assumed for the Kirchhoff approach. As previously mentioned, the expression given by (6) is limited to a number of fundamental assumptions. These conditions can be represented in the FE model by using a two-dimensional, plane strain, Unit Cell model [29]. The model has symmetric (periodic) boundary conditions at the lateral boundaries of its domain (Fig. 3) such that the scattering from a small section of an infinitely long periodic defect can be calculated; provided the width of the cell is significantly larger than the correlation length. The width of the Unit cell is set to be equal to 10 λ_0. This is deemed to be sufficiently wide so as to include an accurate

representation of the surface, yet not so wide as to drastically increase the computational size of the model. The Unit Cell model can provide a good representation of the reflection behaviour of the infinitely wide case, hence, the FE model assumptions are essentially the same at those used in (6), except for the nature of the solver itself.

The model is set up such that all scalar quantities (including defect roughness, σ) can be expressed as a function of the incident wavelength. Thus, the results are shown for an excitation frequency of $1Hz$, in a material in which the bulk velocities are 2 and 1 units for compression and shear waves respectively, with a triangular the mesh discretised at 30 nodes per incident wavelength. Forcing along the nodes of the excitation line (Fig. 3) represents the generation of an infinitely wide plane wave at normal incidence to the rough surface.

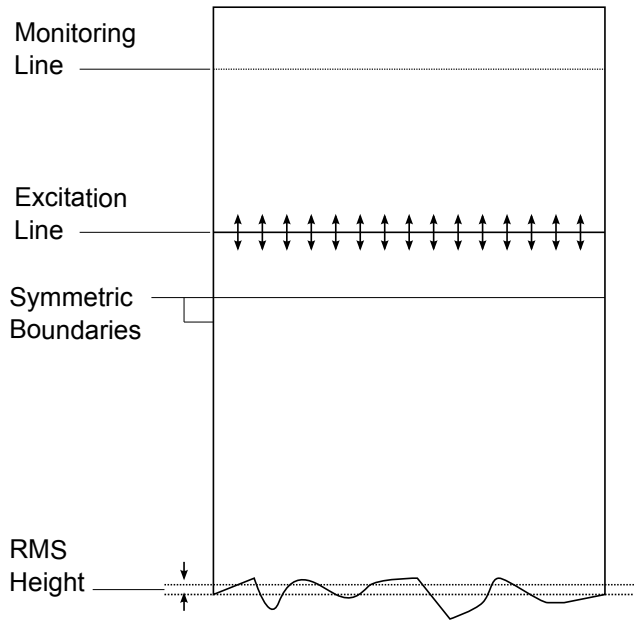

Fig. 3: Unit Cell FE model with symmetric boundaries to simulate an infinite periodic surface, used to calculate the elastic wave scattering of a normally incident compression wave. The model is repeated for multiple realisations of defects defined by the same statistical class of roughness. The signal is monitored parallel to the plane of the incident wave along a monitoring line.

The signal is monitored parallel to the plane of the incident wave at range that is sufficient to distinguish between the reflected compression and shear wave modes. A plane wave solution is obtained by averaging the response along the length of the monitoring line to produce a single time history for the response from the rough surface.

III. Results from normal incident inspections

The FE model considers twenty classes of roughness within a range from $\sigma = 0.017\lambda_{inc}$ up to and including a value of $\sigma = 0.340\lambda_{inc}$. For each class, multiple realisations of defects all defined by the same statistical class are processed using the Unit Cell model. The number of realisations required to calculate the mean signal attenuation is dependent upon the class of defect roughness. When defect roughness is low, the number of realisations required for a convergent solution is less than for greater degrees of roughness, therefore surface realisations are considered until a convergent solution has been obtained. Results from the convergence study are discussed and compared to work presented by Zhang $et\ al$, [13], who discusses converging solutions obtained from Kirchhoff theory simulations.

A. Coherent signal amplitude

To extract the coherent signal amplitude the responses from each defect realisation within the statistical class of roughness must be superposed, as governed by (7).

$$\phi^{\sigma}_{coh} = \frac{\sum_{i=1}^{N} \phi^{\sigma}_{i}}{N} \tag{7}$$

Where ϕ^{σ}_{i} denotes the scattering response from an individual surface realisation i, within the statistical class of defect surface roughness, σ, for the total number of realisations for that class of roughness, N.

By summing the responses from each defect realisation within the statistical class, the effects of superposition cause any out-of-phase artefacts that are inconsistent across all the surfaces to be canceled out. What remains is the in-phase coherent signal which is common to all surfaces within that class of roughness. Using (7), the reduction in coherent signal amplitude for the rough surface with respect to the smooth surface becomes

$$\frac{|\phi^{\sigma}_{coh}|}{|\phi^{\sigma=0}_{inc}|} = \frac{|\frac{\sum_{i=1}^{N} \phi^{\sigma}_{i}}{N}|}{|\phi^{\sigma=0}|} \tag{8}$$

where $\phi^{\sigma=0}$ is the scattering response from a smooth defect with $\sigma = 0$. Fig. 4 shows the comparison between the analytical solution, (6), and numerical solution, (8).

For low levels of roughness there is excellent agreement between the two techniques. This is as expected, since the FE method provides a highly accurate solution to elastic wave scattering and Kirchhoff theory is known to be a good approximation at low levels of roughness [10].

At high levels of roughness disagreement is observed confirming the pessimism of Kirchhoff theory. Due to the limitations of Kirchhoff theory, scenarios where multiple reflections or surface shadowing occur are not accounted for. An accurate scattering solution is only obtained from the scatterer if the deviation of the surface from flat (over a distance comparable to the incoming wavelength) is small in comparison to the wavelength of the incoming wave [2].

This surface property can be expressed quantitatively as a function of the radius of curvature of the defect, a. The Gaussian nature of the surface means that this parameter is itself defined by a distribution function. It is important to know the minimum value within this spread a_{min}, (defined by the 95^{th} percentile), since these smaller surface artifacts are not considered in the analytical solution [4].

$$a_{min} = \frac{0.1\lambda_0^2}{\sigma} \tag{9}$$

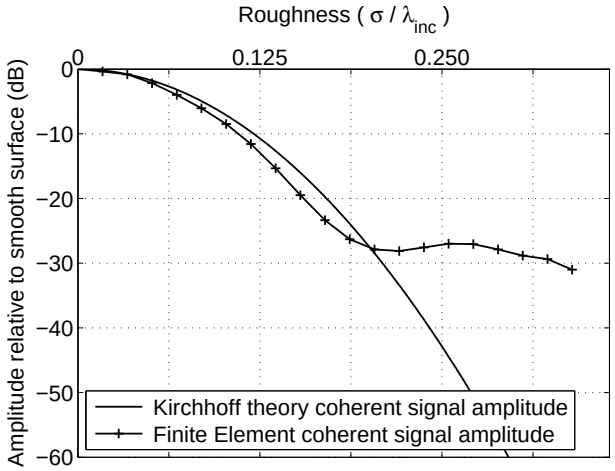

Fig. 4: Reduction of amplitude of wave reflecting from a rough surface, with respect to a perfectly smooth surface. Results shown for coherent component, comparing Kirchhoff theory and Finite Element simulations. Results are for a normally incident compression wave with wavelength λ_{inc}, scattering from a defect with surface roughness, σ.

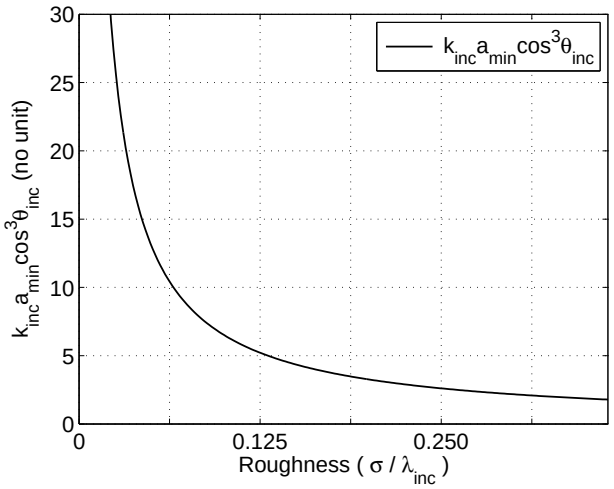

Fig. 5: The variation in the function $k_{inc}a_{min}cos^3\theta_{inc}$ with increasing roughness for a normally incident compression wave, which must be significantly greater than 1 for a valid application of Kirchhoff theory [4].

where λ_0 is the surface correlation length. From (9) it can be seen that a_{min} is inversely proportional to roughness explaining why Kirchhoff theory is no longer valid at high levels of roughness. The accuracy of Kirchhoff theory at high levels or roughness (as described by Bass and Fuks [2]) can be quantitatively expressed by the condition:

$$k_{inc}a_{min}cos^3\theta_{inc} >> 1. \tag{10}$$

which relates the physical size of the radius of curvature, a_{min}, to the incident wavenumber k_{inc} and incident angle θ_{inc}. Combining (9) and (10), allows for a single expression that relates the validity of Kirchhoff theory to defect roughness, (11).

$$\frac{0.1k_{inc}\lambda_0^2 cos^3\theta_{inc}}{\sigma} >> 1. \tag{11}$$

By plotting (10) as a function of roughness, a valid regime of Kirchhoff theory can be identified, Fig. 5.

As roughness increases, this function $k_{inc}a_{min}cos^3\theta_{inc}$ tends to a value of 1. This denotes scenarios where Kirchhoff theory becomes increasingly inaccurate and explains the disagreement at high levels of roughness observed in Fig. 4.

Since multiple realisations of rough surfaces from statistical classes are used to calculate the coherent signal, it is important to understand how many simulations are required to extract the true coherent signal. If too few are considered, not all of the out-of-phase components will have been removed from the scattered signal. However, running an unnecessarily large number of surface realisations, drastically increases computational expense with little benefit to the accuracy of the overall result.

To illustrate this point, the variation in coherent signal amplitude with increasing number of simulations is shown for three classes of roughness, Fig. 6.

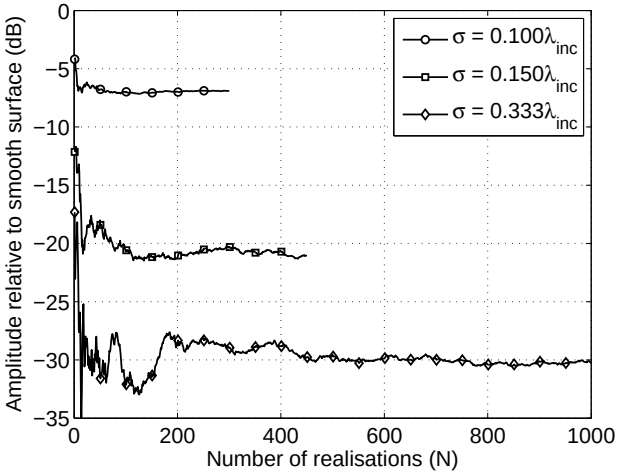

Fig. 6: Variation in coherent signal amplitude with increasing number of surface realisations for three classes of surface roughness to show the number of realisations required to tend towards a convergent result.

The values selected ($\sigma = 0.100\lambda_{inc}$, $\sigma = 0.150\lambda_{inc}$, $\sigma = 0.333\lambda_{inc}$) relate to low, medium and high levels of roughness. It can been seen that for low levels of roughness relatively few realisations are required, typically of the order of a hundred. Little benefit is gained over the accuracy of the reduction of the coherent signal amplitude by running further simulations. For rougher surfaces this is no longer the case. In this instance thousands of surface realisations are required. This results from the increased variation in the surface profile height that can be expected with surfaces that are defined by much larger rms values. It is thought that by extending the crack length, it would be possible to reduce the number of surface realisations required to obtain a convergent solution for the coherent field. However, this would be at the expense

of increasing the computation required to solve each Unit cell. The relationship of such a trade-off has not been considered here.

Studies of simulated reflections from multiple realisations of rough surfaces have previously been considered by Ogilvy, [11], using Kirchhoff theory for acoustic wave scattering and Zhang $et\ al$, [13], using Kirchhoff theory for the elastic case. Zhang also includes the use of a FE model, presenting the scattering from the defect in the form of a scattering matrix. The numerical model is used to identify a valid regime of Kirchhoff theory, concluding that for defects with low levels of roughness, the computational efficiency of the Kirchhoff approach out-weighs the increased accuracy offered by FE. Zhang $et\ al$, [13] also investigates convergence of the total field (not the coherent field) with increasing numbers of simulations. Although different to the coherent field discussed here, the same principles are observed with increasingly rough surfaces requiring a greater number of surface realisations to tend towards convergence. It is also clear that for low levels of roughness, the difference between Kirchhoff theory and FE is small, however, as defect roughness is increased, Kirchhoff theory becomes increasingly inaccurate and a fully numerical approach is therefore required.

B. Total signal amplitude

The convention in dealing with the ultrasonic NDE of rough defects in the power generation industry has been to quantify the reduction of amplitude of the reflection by calculating the expected coherent signal. Of greater practical interest is the mean of the total signal amplitude, which considers both the coherent and diffuse signal amplitudes combined. Multiple realisations must still be considered, but in this instance, instead of superposing the scattering response to obtain a coherent average, the amplitude of the signal from each simulation is obtained, and then the average of these amplitudes is calculated. This removes any dependence of phase variation from the results and instead delivers the value of the amplitude of the reflected signal that would be expected, on average, in an experimental setup. This is the total field, comprising the coherent field and the contribution of the diffuse field in this back-scatter direction. The consideration of the total field that results from the combination of coherent and diffuse fields has been previously reported by Ogilvy using a Kirchhoff theory solution, [4]. The extension made here is to consider a large number of surface realisations with the use of a fully numerical approach.

$$\phi^{\sigma}_{tot} =< |\phi^{\sigma}_{i,N}| > \tag{12}$$

Using (12), the reduction in total signal amplitude due to increasing roughness becomes

$$\frac{|\phi^{\sigma}_{tot}|}{|\phi_{inc}|} = \frac{< |\phi^{\sigma}_{i,N}| >}{|\phi^{\sigma=0}|} \tag{13}$$

Fig. 7 shows the comparison between the analytical solution for the reduction in coherent signal amplitude, (6), and the numerical solution for the reduction in total signal amplitude, (13). Usually, these two signals would not be directly compared, however, as stated earlier, in NDE the inspection of safety critical components has often relied upon the coherent signal amplitude only, as a means to calculate attenuation due to defect roughness. Furthermore, an analytical expression for the total signal amplitude can not be deduced.

The significance of identifying this total field for evaluation is that it is consistent with what is observed when performing an NDE inspection. During an inspection there is normally only a single defect under consideration, therefore there is no means to calculate the coherent signal. On the other hand, the calculation of the amplitude of the total field from multiple realisations of defects of the same statistical description provides the best possible estimate of the expected amplitude: the average value of the amplitude of the received signal for different realisations of such a surface.

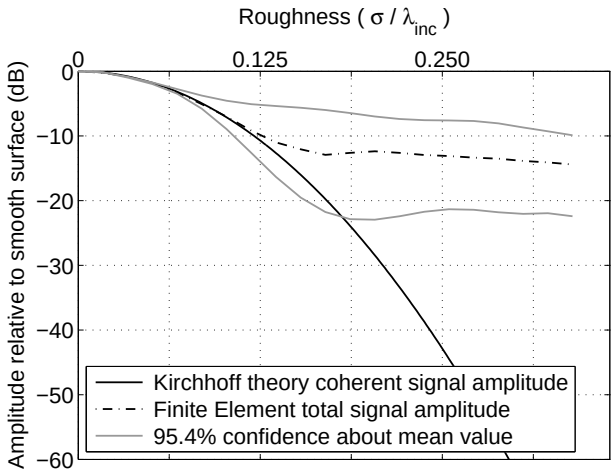

Fig. 7: Comparison between the reduction in signal amplitude for the mean total reflected signal (calculated using FE) and the coherent signal (predicted from Kirchhoff theory). The total reflected signal is plotted with the 95.4% spread (or 2σ confidence) about the mean value.

The results, in Fig. 7, show that as defect roughness is increased, the mean maximum amplitude of the total field is reduced, but not nearly to the same extent as for the Kirchhoff predictions for the coherent field, nor for the FE predictions of the coherent field that were shown in Fig. 4. For defect roughness above $\sigma = 0.125\lambda_{inc}$, the mean reduction in signal amplitude plateaus to a value of approximately $-12.0dB$.

Fig. 7 also shows confidence bands, showing the spread of predicted signal amplitude, that can be applied to this data to indicate the deviation about this mean value. Since multiple realisations of defect roughness are considered, in this process, the uncertainty about the mean reduction can also be shown. As defect roughness increases, the uncertainty in the mean signal amplitude also increases. The confidence bands in Fig. 7 show the 95.4% spread (or 2σ confidence) about the mean value. The confidence bands are calculated using an empirical cumulative density function, which makes no assumptions over the nature of the results or their distribution.

By making comparisons with the coherent signal amplitude

from (6), it can be seen that for low levels of roughness there is excellent agreement between the two techniques. For low levels of roughness, Kirchhoff theory is a very good approximation for the elastic wave scattering. Furthermore, in this region the majority of the total scattered field consists mainly of the coherent scattered field, with the diffuse field still being of relatively low amplitude. However, beyond roughness values of $\sigma = 0.125\lambda_{inc}$ the total measured field and coherent field begin to deviate. This is due to the fact the total field is now comprised of a diffuse scattering component which is increasing with increasing roughness. This confirms the pessimism of Kirchhoff theory for severely rough surfaces and provides a more accurate estimate as to the attenuation in signal amplitude due to defect roughness.

The results discussed here are of importance for practical NDE inspections which are forced to conduct inspections in the high defect roughness regions. Because of the spread in the results, it is difficult to predict what the response from a severely rough defect will be. As previously discussed, the approach taken by industry has been to take an overly conservative approach as outlined by Ogilvy [10], and assume that the reflected back scattered signal from the defect is severely reduced.

The purpose of this approach is to establish a minimum reporting threshold on defects, a level above which the back scattered signal from the defect is deemed unacceptable and action must be taken to address the indication. The approach ensures that all defects of concern are found, but at the expense of drastically increasing the likelihood of oversizing an indication and making subsequent false calls. This in turn results in a large increase in costs due to avoidable periods of extended maintenance or repair.

From Fig. 7 it is possible to establish a new reporting threshold based upon the lower level in the spread of the results (with an associated level of confidence), such that any defect giving a response above this value will be deemed unacceptable. The application of new reporting threshold will significantly reduce the number false calls currently associated with rough defect inspection, removing the overly conservative approach that is currently taken, but without compromising the safety of the inspection.

IV. Oblique incidence backscatter

For oblique incidence, the scattering from rough surfaces is still characterised by the total, coherent and diffuse signals; however, the same attenuation characteristics are not observed. Convention in the power generation industry has been to suggests that for the purposes of NDE, rough surfaces attenuate ultrasonic signals when compared to the equivalent smooth surface for oblique incidence. However, this is not necessarily the case, since the rough surface will still maintain a coherent and diffuse component. This will contribute to the total field since the magnitude of the diffuse signal is greater for rough surfaces than it is for the smooth and is scattered in all directions.

For oblique incidence the combined effect of the coherent and diffuse scattering signals is difficult to assess quantitatively using analytical methods; therefore a numerical approach is applied. This approach is capable of deducing the total scattered field in any desired direction for any incident angle. Furthermore, in the manner applied above to the case of normal incidence, a statistical distribution of results can be obtained to provide the mean signal amplitude from multiple realisations of rough defects from the same statistical class.

Here we consider the effects of defect roughness on the total scattered field for the specific case of back-scatter, that is the field that is scattered back along the path of the incident wave. This case has practical importance for pulse-echo inspections using a single transducer. We consider this case for a range of oblique angles of incidence. In this case an incident shear wave is used, with all spatial dimensions expressed in terms of the incident wavelength. To provide some understanding for the effect of increasing defect roughness for angular performance, these simulations are compiled for two different classes of roughness, $\sigma = 0.063\lambda_{inc}$ and $\sigma = 0.200\lambda_{inc}$. The amplitude of the total field is then compared to the smooth defect case.

The oblique incidence case cannot be simulated using the Unit Cell model that was deployed for the normal incidence study. Therefore, in order to satisfy the requirement for a Gaussian representation of the surface roughness, for which the extent of the defect must be significantly larger than the wavelength of the incident wave, the FE model was set up to represent a relatively large spatial domain. This also has the advantage of minimising the influence of the response from the defect tips on the scattering solution, since they are positioned sufficiently far from any interaction with the narrow incident beam. Furthermore, performing multiple realisations, across multiple angles of incidence, for multiple classes of defect roughness, dramatically increases the number of computations required to extract a statistically significant result. For these reasons, the FE model used had to be adapted slightly through the use of a domain linking algorithm [21].

This allows for the FE model to only consider the area immediately surrounding the defect. An algorithm based on Greens' functions is used, linking the wave potentials around the FE domain to any desired location, in this case a position in the far-field of the defect that is back along the propagation path of the incident wave. All other model variables remain consistent with the normal incident case.

The displacements and stresses for the scattered response are recorded by a monitoring box, and are then passed to the domain linking algorithm. Here defect roughness remains fixed whilst the angle of misorientation, θ, is varied from -60^o to 60^o in 10^o increments. This range is limited because greater values of defect tilt drastically increase the size of the FE model. Multiple realisations of the same defect roughness are considered to calculate the mean total field across all angles of incidence. The results are compared to the response from a smooth defect at normal incidence, see Fig. 9.

For smooth defects, increasing the misorientation of the defect results in a reduction of the magnitude of the total ultrasonic signal that is measured back along the path of propagation. The maximum signal is observed at a misorientation of 0^o, which relates to the normal incidence case. The reduction observed is due to the fact that the specularly reflected signal

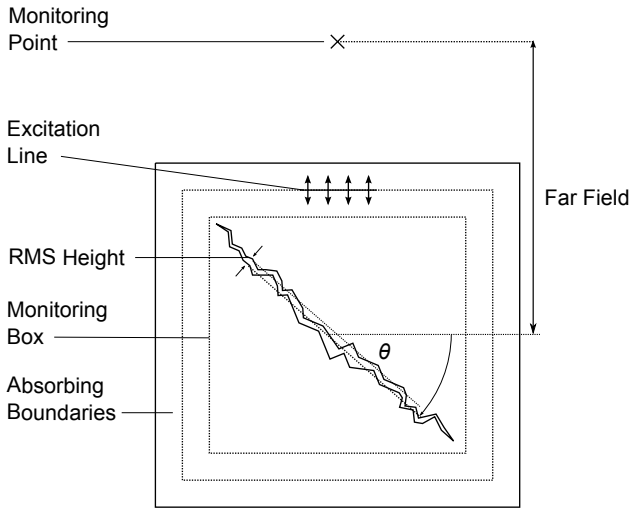

Fig. 8: FE model with significantly reduced spatial domain (model basis from Rajagopal $et\ al$ [21]) for an incident shear wave interacting with a rough defect at oblique incidence where the extent of the defect is greater than the incident beam.

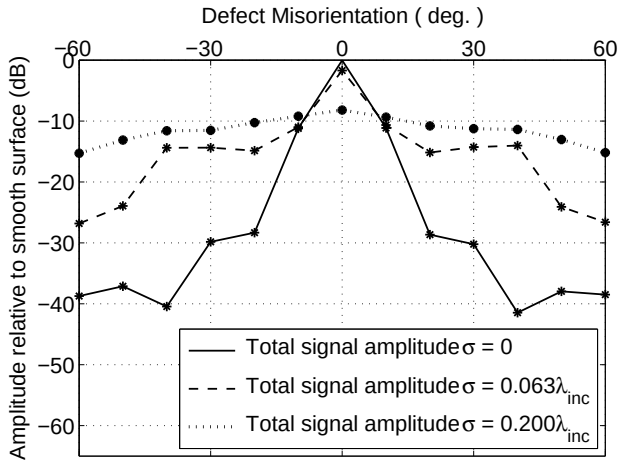

Fig. 9: The mean total reflected signal amplitude as a function of defect misorientation for an incident shear wave. The scattered response for two classes of defect roughness ($\sigma = 0.063\lambda_{inc}$ and $\sigma = 0.200\lambda_{inc}$) is plotted and normalised against the normal incidence case for a smooth defect.

no longer lies along the path of the incident wave. For smooth defects the signal amplitude drops off rapidly, indicating that small degrees of misorientation will hinder the detection of defects. For an infinite smooth crack, it would be expected that response should be zero for angles of misorientation. In this case, the extent of the defect is greater than the width of the incident beam in-order to minimise the influence of the defect tips, however, they still maintain a small contribution to the scattering solution.

For defects with roughness of $\sigma = 0.063\lambda_{inc}$, at 0^o there is an observed reduction in the mean amplitude of the total field, which is consistent with what has been measured in Fig. 7. As the misorientation increases beyond 10^o, the mean amplitude of the total field is again reduced, however, the reduction in signal amplitude is less than what is observed for the smooth case. This is due to an increase in the diffuse scattered field, which is a dominant component of the total scattered field measured back along the path of the incident wave.

As defect roughness is increased further still, as is seen for $\sigma = 0.200\lambda_{inc}$, the same trends are observed. Again at 0^o there is an observed reduction in the mean amplitude of the total field and as the misorientation increases, the amplitude of the total field is again reduced. But in this case for angles of misorientation greater than 10^o, the increase in roughness results in an increase in the diffuse component of the scattered field and therefore a higher amplitude signal than for the smooth and $\sigma = 0.063\lambda_{inc}$ cases.

For defects with misorientation greater than 10^o, defect roughness will increase the magnitude of the back-scattered signal back along the path of propagation, when compared to the same response from a smooth defect, with the same misorientation.

V. Experimental validation

The methodology is validated by comparisons with two experiments, one involving a simple regular profile that can be studied in a deterministic non-statistical manner, and the other involving a real rough surface that is studied statistically.

A. Simple regular profile

A rectangular test piece of thickness $10.0mm$ with a sinusoidal artificial defect machined into the back face is scanned from the opposite face in contact using couplant to couple the ultrasound to the test piece. The test piece is made of 304L Stainless Steel. The sinusoidal back-wall, Fig. 10, is corrugated such that the surface profile varies in one direction only, with a value of $\sigma = 0.220\lambda_{inc}$. Either side of the sinusoidal defect the back-wall is smooth, this is used to normalise the response from the rough surface to that from a smooth surface, so that the results can be presented in the conventional manner as the reduction of amplitude caused by roughness. The sample is scanned from the front face with a $5MHz$, $0.25''$ diameter compression wave transducer at normal incidence.

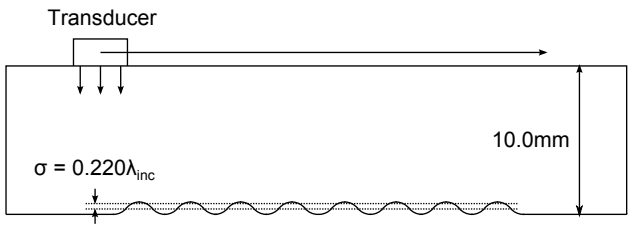

Fig. 10: Sinusoidal-surface test piece used to validate elastic scattering from rough surface. This sample is scanned from the front face with a $5MHz$, $0.25''$ diameter compression wave transducer at normal incidence; this scan is then replicated in FE.

The significance of this sample is that it is a well understood scatterer that can be represented by two-dimensional plane-strain models used in both the Kirchhoff theory and FE approaches. Furthermore, because the sample is sinusoidal, the value of σ remains constant across the surface of the defect.

A pulse-echo configuration is deployed in both the experiment and the modelling, such that the monitored response is a single time history at a position above the defect. The transducer scans along the sinusoidal sample extracting the pulse-echo time history at $1.0mm$ increments. The signals from the flat back-wall on each side of the defect are used to normalise the signals at every rough surface scan position. The experimental approach is replicated in FE by computing individual simulations at every scanning position. The scan results from the experimental and FE simulations are shown in Fig. 11a) and 11b) respectively. A time domain window is used to remove transducer ring-down for the experimental results. A $0.7\mu s$ delay is added to the FE model results to calibrate them against the experimental results. This time difference is due to the delay associated experimentally with imitating the ultrasonic pulse, and it being coupled and transfered into the material.

Figures 11a) and 11b) show good agreement. The time of arrival of the reflected signals are consistent with one another, with both showing similar patterns of reduction of the signal amplitude due to roughness. The response from the smooth back-wall can be seen at scanning positions $0.0mm$ and $37.0mm$. To better appreciate the reduction in signal amplitude due to roughness, the maximum response within the time window $3.9\mu s$ to $5.0\mu s$ is plotted against scanning direction, Fig. 12.

There is excellent agreement between the experiment and the simulations, with the FE model accurately predicting the reduction in the scattered amplitude due to roughness. The mean measured reduction due to roughness is $-9.9dB$, with FE slightly over estimating the reduction ($-11.0dB$).

The previously used approximate Kirchhoff theory solution, Fig. 2, for this problem predicts a reduction of $-33.4dB$. Here, the FE approach for the generic case of this level of roughness, shown in Fig. 7, predicts a reduction of $-12.6dB$, showing that this approach provides a far more accurate representation.

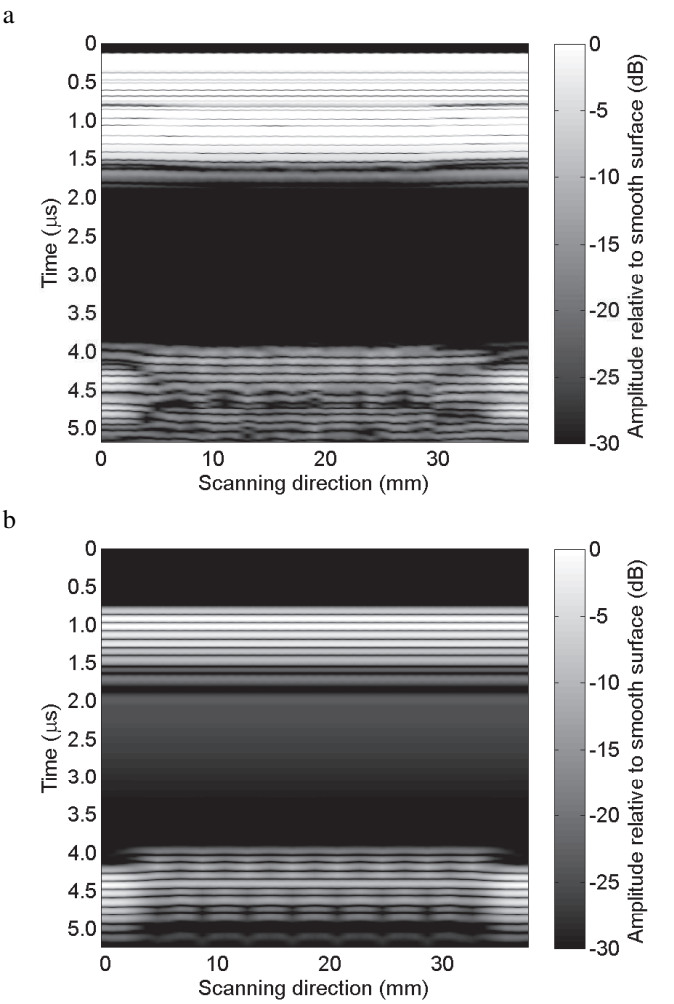

Fig. 11: Figure to show a) Experiential scan and b) FE scan of sinusoidal test piece showing (grey scale) reduction in signal amplitude due to roughness; scans are normalised against the response from the smooth back-wall at $0.0mm$ and $37.0mm$. The response from the sinusoidal section has an arrival time of $3.9\mu s$ and is followed by the response from the smooth section at $4.1\mu s$.

B. Real rough surface

The FE model presented here is a two-dimensional plane-strain representation of elastic scattering from rough surfaces. To check the validity of this approach, the attenuation due to defect roughness shown in Fig. 7, is compared against experimental data.

Four ferritic alloy A533b rectangular test blocks of length $60.0mm$, breadth $40.0mm$ and thickness $40.0mm$ have been produced with back-walls which have roughness varying in both dimension. In each case, the roughness of the back-wall has been generated by a combination of cyclic loading and tearing which has resulted in three types of cracking; fatigue, ductile tear and brittle fast fracture. The rough back-walls are scanned using an Alicona microscope (model number ALC13) to give an highly resolved measurement of their surface profiles ($25\mu m$ spatial discretisation). From these profiles, measurements of surface roughness can be made.

The test blocks are raster scanned from the front face in contact using couplant to couple the ultrasound to the test piece. The scan increments at $1.0mm$ steps with a $4MHz$, $0.5''$ diameter, unfocused compression wave transducer at normal incidence. The roughness of the back-wall varies in two directions and as a result contains a distribution of rms values. A small section of the back-wall is smooth which is used to normalise the responses to established reduction in signal amplitude due to roughness, Fig. 13.

For each increment over the surface, a single time history is obtained. Each time history shows the reduction in signal amplitude of the back-wall signal due to roughness. This reduction varies over different scanning positions due to local variations in surface roughness across the sample. From the surface profile data, the local rms of the surface for the area

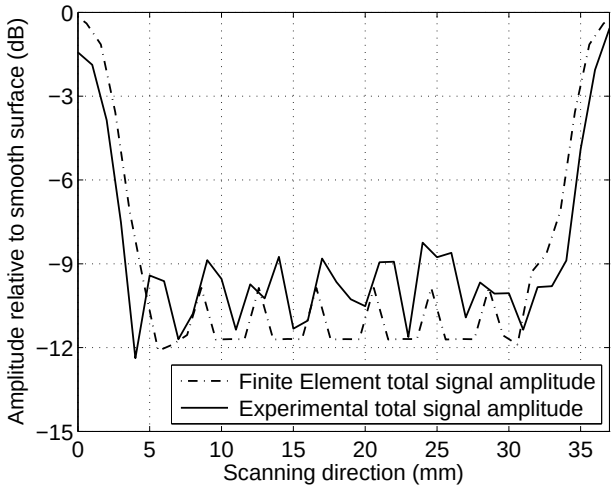

Fig. 12: Reflection coefficient from a scan over sinusoidal surface, showing comparison between experimental measurements and FE simulations.

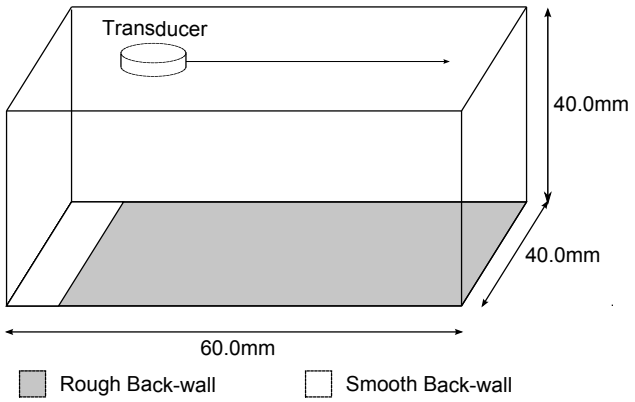

Fig. 13: Dimensions of test blocks and the position of the rough back-wall relative to the scanning surface.

immediately beneath the transducer can be calculated. The local rms is calculated using an area that would have been equivalent to profile of the transducer on the back face. No weighting is applied to surface to compensate for any effects of beam spread. Combining this local rms value of the surface with the reduction in signal amplitude (compared to a smooth back-wall) gives an experimental measurement of the reduction in signal amplitude due to increasing roughness. Across the four samples, 4396 discrete experimental measurements have been taken. Scan positions that are close to the test block edges have been omitted since the effect of the edge of the test block on the scan data is unknown.

Fig. 14 shows a comparison between predictions made using the FE model and the experimental data points. As predicted with the FE model, rough surfaces with the same level of roughness show a spread in the reduction in signal amplitude, this being due to the unique nature of each surface within the statistical class.

The measurements taken experimentally show a plateau in signal attenuation as roughness is increased. This suggests that

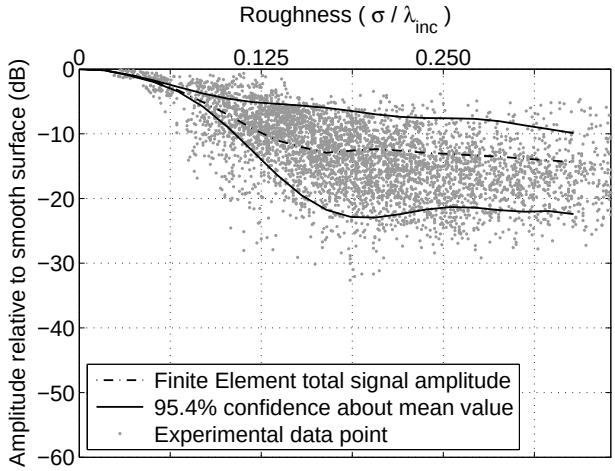

Fig. 14: Comparison between the reduction in reflection coefficients for the mean total reflected signal (calculated using FE) and the total reflected signal measured experimentally. The mean total reflected signal is plotted with the 95.4% spread (or 2σ confidence) about the mean value.

increasing the roughness further will have no effect on the mean attenuation or the confidence in the spread of data.

From the 95.4% spread (or 2σ confidence), by definition it is expected that 2.3% of the experimental data points would lie beneath the lower confidence level. Here, 14.1% of the data points were found to lie below this line. The largest difference between the FE model and the experimental data is at mid-roughness values in the range $\sigma = 0.050\lambda_{inc}$ to $\sigma = 0.167\lambda_{inc}$. The mean attenuation is still applicable, however, experimentally an increase in the spread of values is observed. Therefore, the lower confidence band in this range for the FE model is optimistic. This discrepancy could be attributed to the FE model not considering the response of the transducer or inconsistencies of coupling across the extent of the scanning surface. The use of a two-dimensional model has been justified and remains consistent with approximations imposed on the solution derived from Kirchhoff theory [10], however, the experimental configuration will only truly be represented by a three-dimensional model. At this stage it is unclear what differences would arise. It is expected that the introduction of an additional dimension of roughness would cause scattering to occur out of the plane in three-dimensions. This would lead to a difference between the two and three-dimensional cases and perhaps a further reduction in the expected back-scattered signal. FE models could be re-run to be more representative of the exact system that has been measured experimentally, however the agreement in general is very good, and it is not considered worthwhile to pursue such details.

From all the experimental data points, only 0.1% had a signal attenuation that was less than $-30.0dB$. Practically this implies that the likelihood of encountering a defect that would attenuate the signal amplitude this severely is rare. Furthermore, the statistical nature of this problem means that encountering a crack with such a high signal attenuation across

the entire crack surface is even less likely.

VI. Conclusions

Defects which possess rough surfaces greatly affect ultrasonic wave scattering behaviour, often reducing the magnitude of reflected signals. Ultrasonic NDE inspections of safety-critical components rely upon this response for detecting and sizing flaws. Reliable characterisation is crucial, so it is essential to find an accurate means to predict any reductions in signal amplitude. Kirchhoff theory has been the tool of choice for modelling elastodynamic scattering problems from complex geometrical scatterers, however, it has been widely recognised that this approach often over estimates signal attenuation, especially for high levels of roughness. A numerical method, such as a FE model, does not suffer the same limitations as an analytical technique and offers the potential to calculate a fully elastic solution to the scattering from rough surfaces.

Here, the application of FE models to calculate the elastic scattering from multiple realisations of defects within a statistical class of roughness for normal and oblique incidence is used. Results from the FE models were compared with Kirchhoff theory predictions and experimental measurements in order to establish confidence in the new approach.

At low roughness excellent agreement was observed, whilst higher values confirmed the pessimism of Kirchhoff theory. Furthermore, the mean total signal amplitude was calculated, which is more representative of the information obtained during an NDE inspection. Reductions in the total signal amplitude due to increasing roughness have been found to be significantly less than indicated by the coherent signal component alone.

The numerical model was extended to consider the response for oblique incident cases. It has been shown that for defect misorientation greater then 10^o, as defect roughness increases the total scattered field reflected in the direction that is back along the path of the incident signal is increased when compared to the smooth defect case.

The validity of the FE model has been assessed by comparing the predicted attenuation in signal amplitude due to roughness, to that measured on experimental samples. Good agreement between the FE and experimental data was demonstrated. The 95.4% spread (or 2σ confidence) from the FE model has been shown to be narrower than the spread measured experimentally, however, the mean attenuation in the total field amplitude is consistent with the experimental data points.

The results from this study present a significant improvement that can be used directly for the benefit of inspections in industry. The analysis provides a robust basis for a less sensitive, yet safe, threshold for inspection of rough defects in safety critical components.

Acknowledgment

The authors would like to acknowledge the EPSRC, the UK Research Centre for NDE (RCNDE) and Dr. Jill Ogilvy for their help and support with this research. Additional thanks are also given to the mathematics department of Imperial College London, EDF R&D and AMEC for useful discussions, expertise and provision of samples.

References

[1] F. Gilbert and L. Knopoff, "Seismic scattering from topographic irregularities," *J. Geophys. Res.*, vol. 65, no. 10, pp. 3437–3444, 1960.

[2] F. G. Bass and I. M. Fuks, *Wave scattering from statistically rough surfaces*. Pergamon Press, Oxford, 1979.

[3] Lord Rayleigh, *The Theory of Sound*, 1st ed. London: Macmillan, 1878, vol. 2.

[4] J. A. Ogilvy, *Theory of wave scattering from random rough surfaces*. Institute of Physics Publishing, 1991.

[5] J. D. Achenbach, L. Adler, D. Kent Lewis, and H. McMaken, "Diffraction of ultrasonic waves by penny-shaped cracks in metals: Theory and experiment," *J. Acoust. Soc. Am.*, vol. 66, no. 6, pp. 1848–1856, 1979.

[6] R. K. Chapman, "Ultrasonic scattering from smooth flat cracks: an elastodynamic Kirchhoff diffraction theory," *CEGB report, North Western Region NDT Applications Centre NWR/SSD/84/0059/R*, 1984.

[7] R. K. Chapman, "A system model for the ultrasonic inspection of smooth planar cracks," *J. Nondestruct. Eval.*, vol. 9, no. 2-3, pp. 197–210, 1990.

[8] A. L. Lopez-Sanchez, Hak-Joon Kim, L. W. Schmerr Jr., and A. Sedov, "Measurement models and scattering models for predicting the ultrasonic pulse-echo response from side-drilled holes," *J. Nondestruct. Eval.*, vol. 24, no. 3, pp. 83–96, 2005.

[9] J. A. Ogilvy, "An estimate of the accuracy of the Kirchhoff approximation in acoustic wave scattering from rough surfaces," *J. Phys. D: Appl. Phys.*, vol. 19, no. 11, pp. 2085–2113, 1986.

[10] J. A. Ogilvy, "Theoretical comparison of ultrasonic signal amplitudes from smooth and rough defects," *NDT Int.*, vol. 19, no. 6, pp. 371–385, 1986.

[11] J. A. Ogilvy, "Model for the ultrasonic inspection of rough defects," *Ultrasonics*, vol. 27, no. 2, pp. 69–79, 1989.

[12] S. F. Burch, N. Collett, R. K. Chapman, and M. W. Toft, "Experimental validation of the TRANGLE and related NDT codes for modelling the ultrasonic inspection of rough cracks," *Insight*, vol. 46, no. 2, pp. 74–76, 2004.

[13] J. Zhang, B. W. Drinkwater, and P. D. Wilcox, "Longitudinal wave scattering from rough crack-like defects," *Ultrasonics, Ferroelectrics and Frequency Control, IEEE Transactions on*, vol. 58, no. 10, pp. 2171–2180, 2011.

[14] J. Zhang, B. Drinkwater, and P. Wilcox, "Effect of roughness on imaging and sizing rough crack-like defects using ultrasonic arrays," *Ultrasonics, Ferroelectrics and Frequency Control, IEEE Transactions on*, vol. 59, no. 5, pp. 939–948, 2012.

[15] M. Israeli and S. A. Orszag, "Approximation of radiation boundary conditions," *J. Comp. Phys.*, vol. 41, no. 1, pp. 115–135, 1981.

[16] M. Castaings, C. Bacon, B. Hosten, and M. V. Predoi, "Finite element predictions for the dynamic response of thermo-viscoelastic material structures," *J. Acoust. Soc. Am.*, vol. 115, no. 3, pp. 1125–1133, 2004.

[17] M. Castaings and C. Bacon, "Finite element modeling of torsional wave modes along pipes with absorbing materials," *J. Acoust. Soc. Am.*, vol. 119, no. 6, pp. 3741–3751, 2006.

[18] W. Ke, M. Castaings, and C. Bacon, "3D finite element simulations of an air-coupled ultrasonic NDT system," *NDT&E Int.*, vol. 42, no. 6, pp. 524–533, 2009.

[19] P. Rajagopal, M. Drozdz, E. A. Skelton, M. J. S. Lowe, and R. V. Craster, "On the use of absorbing layers to simulate the propagation of elastic waves in unbounded isotropic media using commercially available finite element packages," *NDT&E Int.*, vol. 51, pp. 30–40, 2012.

[20] J. R. Pettit, A. Walker, P. Cawley, and M. J. S. Lowe, "A Stiffness Reduction Method for efficient absorption of waves at boundaries for use in commercial Finite Element codes," *Ultrasonics, in press*, 2014.

[21] P. Rajagopal, E. A. Skelton, W. Choi, M. J. S. Lowe, and R. V. Craster, "A generic Hybrid model for bulk elastodynamics, with application to ultrasonic Nondestructive Evaluation," *Ultrasonics, Ferroelectrics and Frequency Control, IEEE Transactions on*, vol. 59, no. 6, pp. 1239–1252, 2012.

[22] S. Mahaut, N. Leymarie, C. Poidevin, T. Fouquet, and O. Dupond, "Study of complex ultrasonic NDT cases using hybrid simulation method and experimental validations," *Insight*, vol. 53, no. 12, pp. 664–667, 2011.

[23] P. D. Wilcox and A. Velichko, "Efficient frequency-domain finite element modeling of two-dimensional elastodynamic scattering," *J. Acoust. Soc. Am.*, vol. 127, no. 1, pp. 155–165, 2010.

[24] W. D. Smith, "The application of finite element analysis to body wave propagation problems," *Geophys. J. R. Astron. Soc.*, vol. 42, no. 2, pp. 747–768, 1975.
[25] R. Ludwig and W. Lord, "A finite-element formulation for the study of ultrasonic NDT systems," *Ultrasonics, Ferroelectrics and Frequency Control, IEEE Transactions on*, vol. 35, no. 6, pp. 809–820, 1988.
[26] M. S. Longuet-Higgins, "Statistical properties of an isotropic random surface," *Phil. Trans. R. Soc. A*, vol. 250, no. 975, pp. 157–174, 1957.
[27] J. A. Greenwood, "A unified theory of surface roughness," *Proc. R. Soc. A*, vol. 393, no. 1804, pp. 133–157, 1984.
[28] W. Schmerr, *Fundamentals of ultrasonic NDE - A modelling approach*. Plenum Press, New York, 1998.
[29] W. Choi, E. Skelton, M. J. S. Lowe, and R. Craster, "Unit cell finite element modelling for ultrasonic scattering from periodic surfaces," in *Rev. Prog. QNDE: VOLUME 32*, ser. AIP Conference Proceedings, vol. 1511, 2013, pp. 83–90.

Dr. James R. Pettit, EngD, MSci James Pettit was born in Stevenage, England in 1987. He received an EngD from the UK Research Centre in Non-Destructive Evaluation, Department of Mechanical Engineering, Imperial College London in 2015 and an MSci degree in Physics from Imperial College London in 2010. He is currently working for Frazer-Nash Consultancy in the Engineering Analysis group.

Dr. Anthony. E. Walker, PhD, CEng, FIMechE, FNucl Anthony (Tony) Walker was born in Sheffield, England 1962. He received a BSc degree in mathematics from the University of Bradford in 1983 and a PhD in Mechanical Engineering from Sheffield Hallam University in 1987. He joined Rolls-Royce Submarines (then Rolls-Royce and Associates) in 1988 working in the non-destructive testing (NDT) group. During this time he played a significant role in the introduction of inspection qualification (validation) of NDT into the submarines programme and is currently working on the development of policy on in-service inspection and structural integrity. He is a Fellow of the IMechE and the Nuclear Institute.

Professor Michael J. S. Lowe, FREng, PhD, CEng, FIMechE, FInstP, FInstNDT Michael Lowe holds a BSc degree in Civil Engineering and MSc and PhD degrees in Mechanical Engineering. He worked in engineering consultancy from 1979 to 1989, specialising in the application and development of numerical methods for the solution of problems in solid mechanics. His principal clients were in the nuclear power and offshore oil industries. Since 1989 he has worked in the Department of Mechanical Engineering at Imperial College London, where his appointment is Professor of Mechanical Engineering. His research expertise is in the use of ultrasound for Non Destructive Evaluation (NDE), with specialist interests in guided waves, the interaction of waves with defects and structural features, and numerical modelling. He has published over 250 journal and conference papers relating to ultrasound, guided waves, numerical modelling and NDE. He was elected Fellow of the Royal Academy of Engineering in 2014 for his research contributions to NDE.